ELSEVIER

Journal of Nuclear Materials 282 (2000) 32–39

journal of nuclear materials

www.elsevier.nl/locate/jnucmat

Comparative study on the fatigue crack growth behavior of 316L and 316LN stainless steels: effect of microstructure of cyclic plastic strain zone at crack tip

Wan-Young Maeng *, Mun-Hwan Kim

Korea Atomic Energy Research Institute, P.O. Box 105, Yusong, Taejon 305–353, South Korea

Received 12 April 1999; accepted 13 August 2000

Abstract

The fatigue crack growth rates in 316L and 316LN stainless steel were measured to compare the resistance to fatigue crack growth of the alloys and to evaluate the effects of nitrogen addition to the alloys. Fatigue crack growth tests were carried out at 1 Hz with a sinusoidal tension stress wave form ($R = 0.2$) between 25°C and 600°C in air. Crack lengths were monitored by direct current potential drop method. 316LN stainless steel showed better crack growth resistance than 316L stainless steel did. The characteristics of the cyclic plastic strain zone of 316L and 316LN stainless steel at the crack tip were analyzed with micro hardness test, the X-ray diffraction method and transmission electron microscopy. The improvement of the fatigue crack growth resistance of 316LN stainless steel is discussed in relation to the degree of crack closure, strain induced martensite transformation and the dislocation structure in the cyclic plastic stain zone at the fatigue crack tip.

PACS: 81.40.N; 71.55.A; 81.30.K; 61.72.F

1. Introduction

316L and 316LN (nitrogen added) austenitic stainless steels are considered as candidates for structural materials in a liquid metal reactor. It was reported by some investigators [1–5] that the addition of nitrogen to austenitic stainless steel improves the tensile and fatigue properties of the alloys including the demostration of nitrogen strengthening by Sandstrom and Berguist [6]. But the roles of nitrogen for the improvement of fatigue properties of the alloys during the fatigue cycle are not clearly understood.

A cyclic plastic strain zone is formed at the fatigue crack tip when a material experiences cyclic fatigue loads. The microstructural behaviors, such as crack closure, residual stress, strain induced phase transformation, and dislocation structures in the fatigue plastic strain zone at the crack tip, are significant factors which determine the fatigue crack growth resistance.

Fatigue crack growth tests were carried out for 316L and 316LN stainless steels to compare the crack growth rate of these two alloys at room temperature and 600°C. And the variations of microstructures in the fatigue plastic zone at the crack tip were discussed in relation to the fatigue crack growth properties of the stainless steels.

2. Experimental method

2.1. Materials

316L (0.04% N) and 316LN (0.14% N) stainless steels were prepared for fatigue crack growth tests for investigating the effects of nitrogen additions to the materials. The chemical composition is shown in Table 1.

* Corresponding author. Tel.: +82-42 868 2295; fax: +82-42 868 2212.

E-mail address: gobul20@nanum.kaeri.re.kr (W.-Y. Maeng).

0022-3115/00/$ - see front matter
PII: S0022-3115(00)00401-3

Table 1
Chemical compositions of 316L and 316LN stainless steel

Element (wt %)	C	Ni	Cr	Mn	P	S	Si	Mo	N
316L	0.020	11.21	17.38	1.86	0.027	0.0054	0.51	2.36	0.038
316LN	0.018	11.23	17.58	1.67	0.021	0.0008	0.46	2.79	0.14

Specimens were fabricated from plates of 316L and 316LN stainless steels which were solution annealed at 1373 K for 1 h and water quenched after hot rolling.

2.2. Fatigue crack growth tests

Fatigue crack growth tests were carried out on 316L and 316LN stainless steel samples at room temperature and 600°C. Compact tension (CT) type specimens of 5 mm thickness with no side grooves, having the shape and dimension as shown in Fig. 1, were used for the fatigue crack growth tests. The notches of the specimens were machined with a wire cutter and the surface of the specimens was polished with 600 grit polishing paper. All the specimens were fatigue precracked to provide a sharpened fatigue crack. Precracking of fatigue crack propagation specimens was accomplished using a stepwise ΔK-decreasing procedure to obtain an initial crack length of 1.5 mm before staring the fatigue crack growth rate (FCGR) measurements. Tests were carried out according to ASTM E647. Cyclic fatigue loads between 0.78 kN (80 kgf) and 3.92 kN (400 kgf) with a frequency of 1 Hz were applied with an Instron tensile test machine. The direct current potential drop (DCPD) method was used to measure fatigue crack length.

2.3. Crack closure measurement

The closure load was determined by finding the inflection point on the load vs. load-line displacement curve during fatigue crack growth tests. This was done by detecting the point on the loading side of the curve that has the same slope as the elastic unloading segment on the unloading side of the curve.

2.4. Microhardness test

Microchardness measurements around the crack tip in the fatigue fractured specimens were used to analyze the plastic zone distribution on the fatigue fracture surfaces.

The specimens for microhardness measurements were prepared by sectioning the fatigue tested specimens with a diamond cut off wheel in the direction shown in Fig. 2, at the crack lengths corresponding to ΔK values of 21, 28 and 40 MPa $\sqrt{\text{m}}$. The sectioned suface was carefully ground and polished with paste of 0.05 μm diamond particles. At each sectioned surface which is perpendicular to the plane of fracture, hardness indentations were carried out in direction Y along the half thickness line as shown in Fig. 2. The microhardness measurements were made with an HMV-2000 microhardness tester (Shimadzu) with a load of 25 g and loading time of 15 s. The tip of the indenter is a diamond in the form of a right

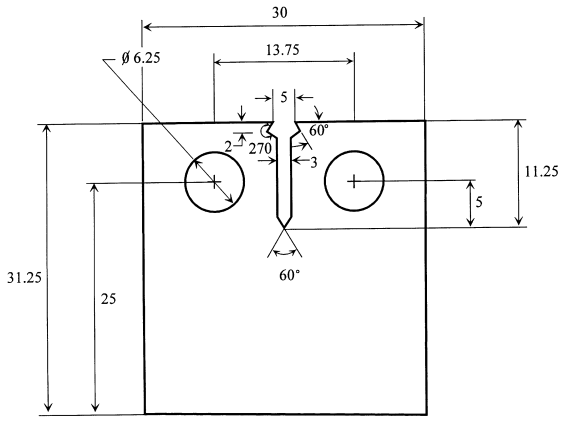

Fig. 1. Dimension of the compact tension specimen in this study.

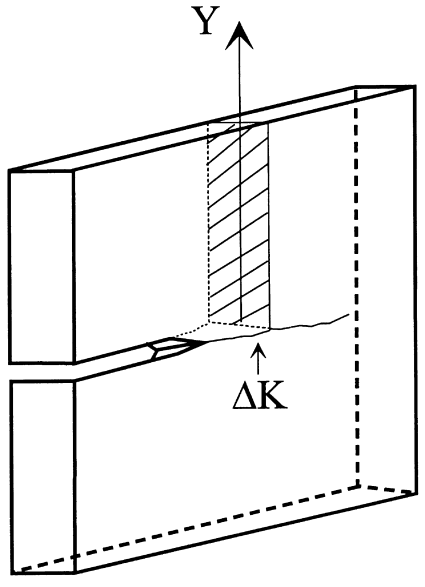

Fig. 2. Schematic drawing of the cutting of a compact tension specimen for one level of the stress intensity factor (ΔK).

pyramid with a square base having the angle of 136° between the opposite faces at the vertex. The hardness (HV) was determined based on the test load and the indentaion area calculated from the indented diagonal length in this relation

$$HV = 1.854F/d^2,$$

where HV is the Vickers hardness, F the test load (kgf) and d is the mean of the indentation diagonal length (mm).

2.5. X-ray diffraction

Strain induced martensites formed during the fatigue crack propagation tests on the fracture surface of 316L and 316LN stainless steel specimens (tested at 25°C and 600°C, were investigated by X-ray diffration. X-ray diffractions were carried out for 2θ from 20° to 100°. Co K_α radiation was used and the standard correction was employed.

2.6. Dislocation structure by transmission electron microscopy (TEM)

After the fatigue crack growth tests, the specimens were sectioned and 3 mm disks were extracted as indicated in Fig. 3. Thin foils were prepared by electropolishing the 3 mm disks in a twin jet electropolisher, using the mixed solution $HCIC_4 : CH_3COOH : C_2H_5OH = 1 : 4 : 1$) at 3°C and 25 V DC. The foils were then observed in a transmission electron microscope at 200 kV. The 3 mm disks for TEM observation were extracted from locations with similar ΔK in the 316L and 316LN stainless steels from an area between 10 and 20 mm of the crack length, to avoid the effect of the machined notch and to ensure stable fatigue crack growth conditions. The regions observed in the TEM corresponds to a zone at a ~200–300 μm depth from the fracture surface in the underlying cyclic plastic strain zone in the wake of the crack tip.

3. Experimental results

3.1. Fatigue crack growth

The fatigue crack growth rates of 316L and 316LN stainless steels at room temperature were shown as a function of ΔK in Fig. 4. The fatigue crack growth rate of 316LN stainless steel is slower than that of 316L stainless steel in the ΔK range of 20 to 50 MPa$\sqrt{\text{m}}$, as shown in Fig. 4. The crack growth data of Vogt [3] also show a similar trend. 316LN stainless steel also has a better resistance to fatigue crack growth than 316L stainless steel at 600°C, as shown in Figs. 5 and 6. The fatigue crack lengths of 316L and 316LN stainless steel at 600°C, as a function of fatigue cycles, are shown in Fig. 5. As an example, a crack about 6.5 mm in length in 316L stainless steel grows more rapidly than the crack of similar length in 316LN stainless steel does, as shown in Fig. 5. The trend of rapid crack growth in 316L stainless steel in Fig. 5 is also reflected in Fig. 6. The fatigue crack growth rates (da/dN) of 316L and 316LN stainless steel as a fucntion of stress intensity range (ΔK) at 600°C were shown in Fig. 6. As ΔK increases, crack growth rate increases more rapidly in 316L stainless steel than in 316LN stainless steel. It is clear that the resistance to fatigue crack growth in 316LN stainless steel is better than in 316L stainless steel at a high ΔK range at 600°C.

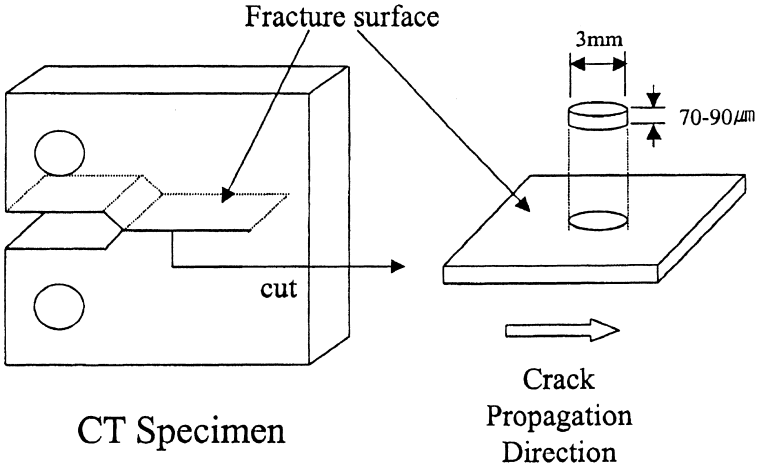

Fig. 3. TEM specimens preparation for observation of the dislocation structures in cyclic plastic zone at fatigue crack tip.

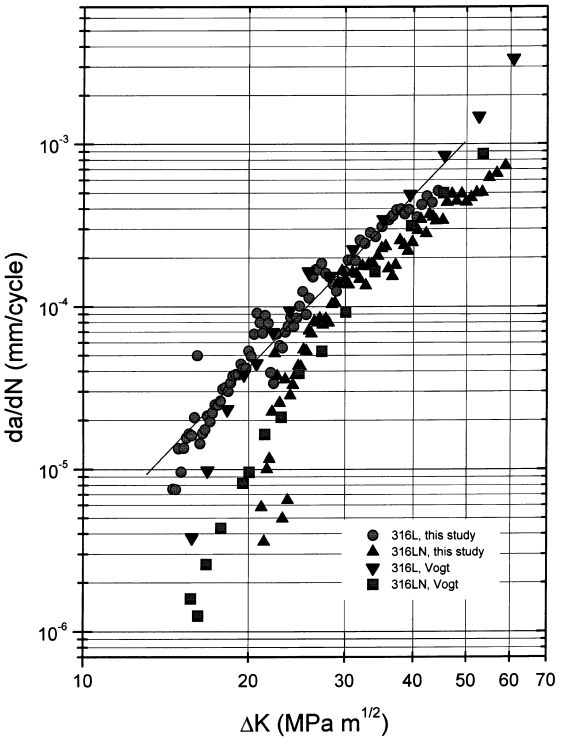

Fig. 4. Fatigue crack growth rates (da/dN) of 316L and 316LN stainless steels as a function of ΔK at room temperature.

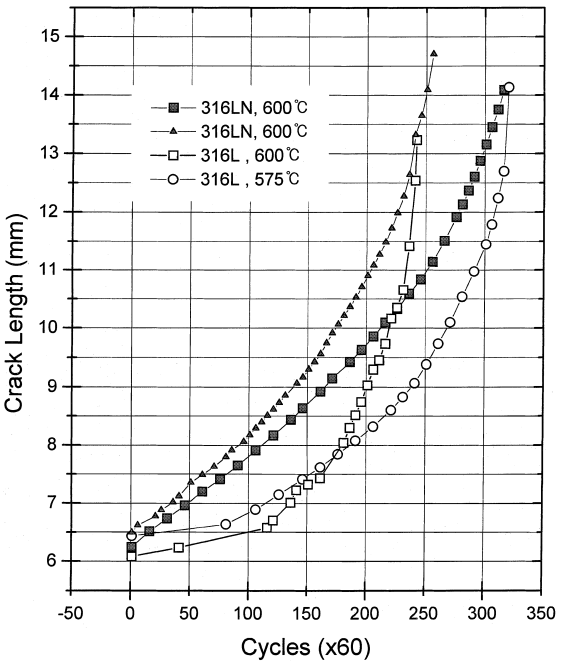

Fig. 5. Fatigue crack length of 316L and 316LN stainless steel as a function of fatigue cycles at 600°C.

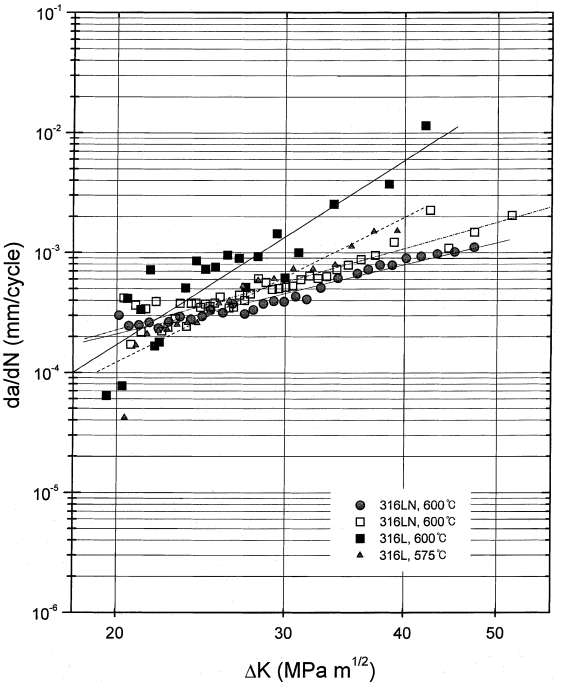

Fig. 6. Fatigue crack growth rates (da/dN) of 316L and 316LN stainless steels as a function of ΔK at 600°C.

3.2. Crack closure

The normalized crack closure loads, $(P_{cl} - P_{min})/(P_{max} - P_{min})$, of 316L and 316LN stainless steels during the fatigue crack growth test at room temperature were compared in Fig. 7 (P_{cl} is the crack closure load; P_{max} the maximum load; P_{min} is the minimum load). 316LN stainless steel has a lower level of crack closure loads than that of 316L stainless steel in the $\Delta K < 25$ MPa$\sqrt{m}$. The crack closure disappears at $\Delta K < 20$ MPa$\sqrt{m}$ in in both alloys. The magnitude of normalized crack closure loads can be related to the significant decrease of the fatigue crack growth rate at $\Delta K < 20$ MPa$\sqrt{m}$ in Fig. 4.

3.3. Micro hardness test

Figs. 8 and 9 show the plots of the hardness readings as a function of distance for the specimens of 316LN and 316L stainless steel in Y-direction of Fig. 2 from the fracture surface. The microhardness increases sharply within the reversed zone in both stainless steels. The two austenitic steels show work hardening near the fatigue crack tip.

Hahn et al. [7] measured the cyclic plastic strain zone dimension using an etch pitting technique and found it to be given by

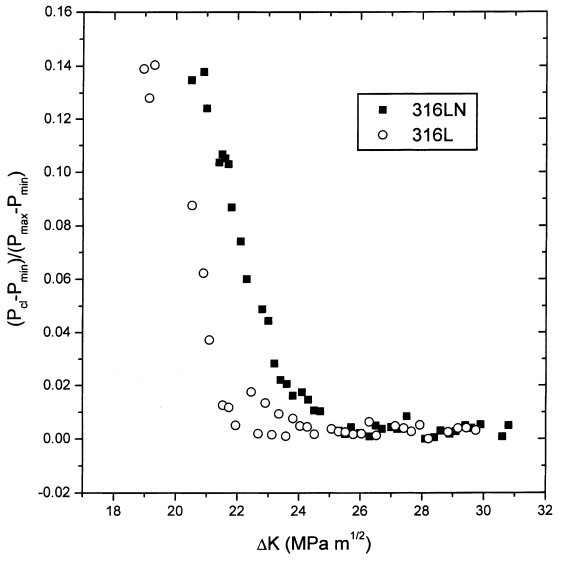

Fig. 7. Normalized crack closure loads, $(P_{cl} - P_{min})/(P_{max} - P_{min})$, of 316L and 316LN stainless steel as a function of ΔK at room temperature.

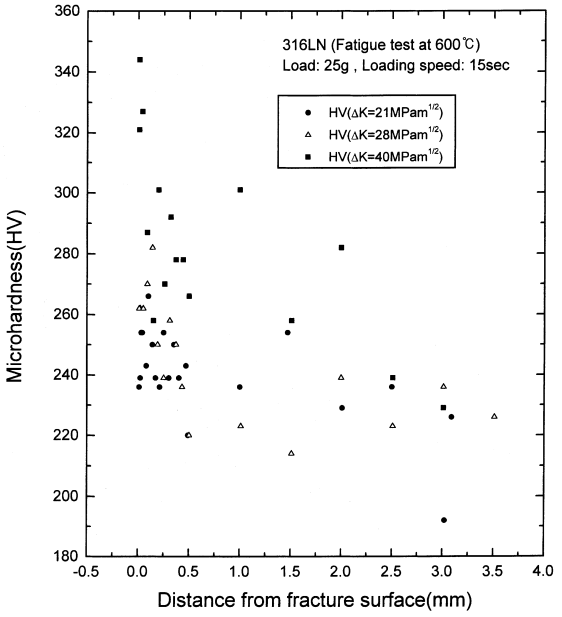

Fig. 8. Microhardness (HV) as a function of distance from fracture surface in 316LN stainless steel specimen tested at 600°C.

$$r_c^y = 0.033(\Delta K/\sigma_y)^2, \quad (1)$$

where r_c^y is the cyclic plastic strain zone when measured in the Y-direction from the crack plane to the elastic–plastic boundary. The size of the cyclic plastic strain

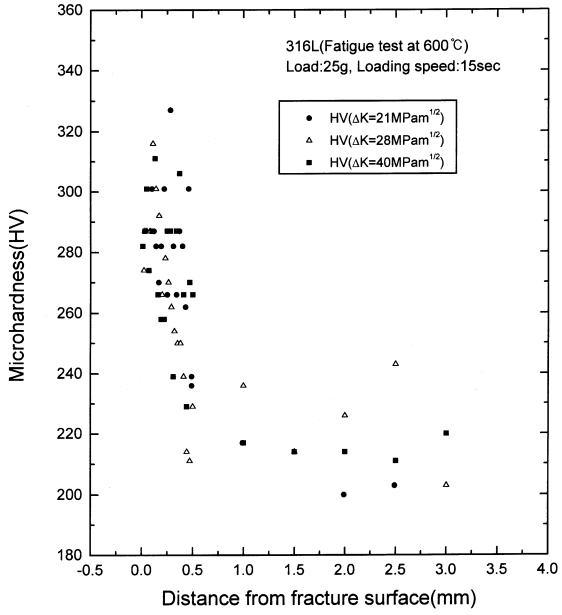

Fig. 9. Microhardness (HV) as a function of distance from fracture surface in 316L stainless steel specimen tested at 600°C.

zone is approximately 1/4 of the monotonic plastic zone size. The transition between the monotonic and the cyclic zone is not well defined in Figs. 8 and 9. The lengths of the cyclic plastic strain zone of 316LN stainless steel are about 0.44, 0.80, 1.62 mm at ΔK of 21, 28 and 40 MPa$\sqrt{\text{m}}$ based on the calculation according to Eq. (1). The measured cyclic plastic strain zone size for 316LN stainless steel based on the microhardness measurements is comparable to the estimation. The zone size of 316L stainless steel also has similar dimensions, as shown in Fig. 9.

3.4. X-ray diffraction analysis for the fracture surface of 316LN stainless steel

X-ray diffraction analysis was conducted for the fatigue fracture surface of 316L and 316LN stainless steels to investigate the formation of strain-induced martensite phase in the cyclic plastic strain zone at the crack tip during fatigue crack growth. The relative amount of martensite phase formed on the fracture surfaces of 316L and 316LN stainless steels was compared by analyzing the relative intensities of the peaks for martensite phase, $\alpha(110), \alpha(200)$ and $\alpha(211)$ in the diffraction patterns of the two stainless steels at various temperature which are shown in Fig. 10. The formation of the martensite phase was confirmed by the presence of the martensite peaks, $\alpha(110), \alpha(200)$ and $\alpha(211)$ in the diffraction patterns for the fracture surface of 316L

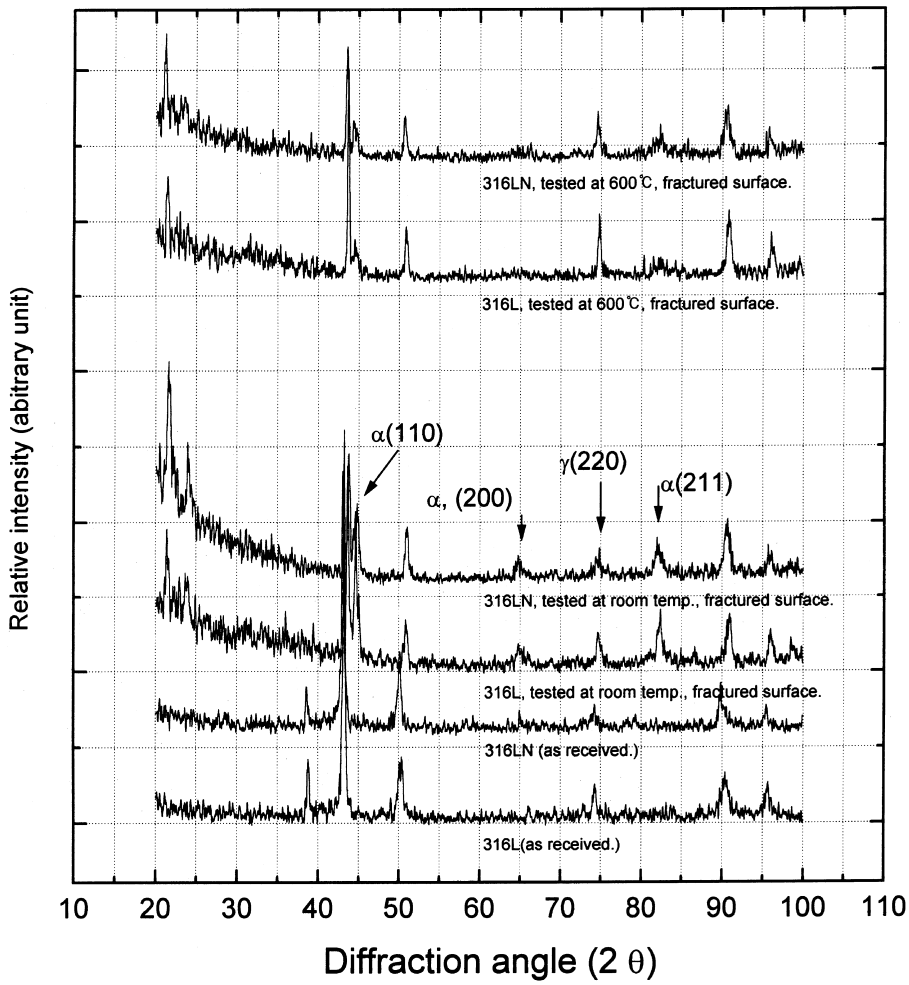

Fig. 10. Results of X-ray diffraction analysis for the fatigue fracture surfaces of 316L and 316LN stainless steels.

and 316LN stainless steels after fatigue crack growth tests at 25°C and 600°C.

3.5. Dislocation structures in fatigue plastic zone

Dislocation structures in the cyclic plastic strain zone of 316L and 316LN stainless steels which were tested at 25°C are shown in Fig. 11. The figures are for the fatigue plastic zone below the fracture plane at ΔK of about 35 MPa$\sqrt{\text{m}}$. There are significant differences in dislocation structures in the fatigue plastic zones of 316L and 316LN stainless steels. The dislocation structure of 316L stainless steel shows a cellular arrangement of dislocation tangles, whereas the dislocation structure of 316LN stainless steel shows a planar arrangement. The figures indicate that the two alloys have very different slip characteristics, and this difference could influence the fatigue resistance of the alloys.

4. Discussion

316LN stainless steel has better resistance to fatigue crack growth than 316L stainless steel does. The improvement in resistance to fatigue crack growth of 316LN stainless steel can be attributed to the following factors at the cyclic plastic strain zone at the crack tip:

1. crack closure behavior,
2. compressive stress induced by martensitic transformation, and
3. cross slip characteristics of dislocation.

4.1. Effect of crack closure

The degrees of crack closure are shown in Fig. 7. Below ΔK of 25 MPa$\sqrt{\text{m}}$, crack closures appear in both 316L and 316LN stainless steels and the magnitude of the crack closures increases as the stress intensity range

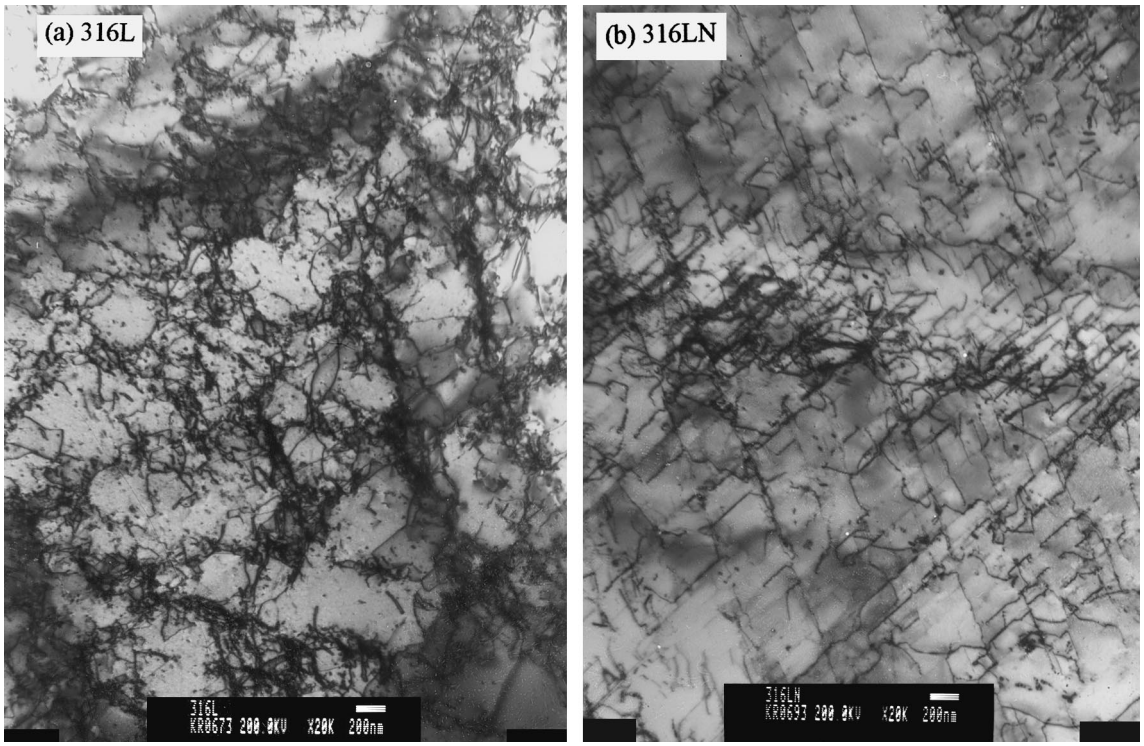

Fig. 11. Dislocation structures in the fatigue plastic zones at crack tip of: (a) 316L, and (b) 316 LN stainless steel.

decreases. The magnitude of the normalized crack closure load in 316LN stainless steel is larger than in 316L stainless steel at $\Delta K > 25$ MPa$\sqrt{\text{m}}$. The fact reflected in Fig. 7 is that fatigue crack growth rate decreases more rapidly in 316LN stainless steel than in 316L stainless steel at $\Delta K > 25$ MPa$\sqrt{\text{m}}$. At $\Delta K > 25$ MPa$\sqrt{\text{m}}$, there is no crack closure in the two alloys. So it seems that crack closure does not have an influence significant enough to induce the difference of the fatigue crack growth resistance between 316L and 316LN stainless steels.

4.2. Effect of strain induced martensitic transformation at crack tip

Austenitic stainless steel experiences strain-induced martensitic transformation when the alloy deforms [8,9]. It was reported that strain induced martensitic transformation increases the resistance to fatigue crack growth. It is explained that the martensitic transformation at the crack tip increases the resistance to fatigue crack growth because of (1) high strain hardening properties [10] and (2) compressive residual stress accompanying phase transformation.

Martensitic transformation at the crack tip increases the strain hardening properties and improves the resistance to plastic flow [11]. The improvement of the resistance to plastic flow decreases the crack growth rate. Head [12] measured the fatigue crack growth rate (da/dN) for 301 steel varying the value of strain hardening properties ($1/\text{UTS} - \sigma_y$). It was confirmed that the fatigue crack growth rate decreased 1/20 when the value of strain harding properties ($1/\text{UTS} - \sigma_y$) increased to the factor of 3 in the alloy.

Martensitic transformation accompanies a volume increase at the crack tip during fatigue crack growth. The increase in volume induces compressive stress in the crack tip area. This compressive stress can reduce the effective stress in the crack tip and induce a strengthening effect [13,14].

The existence of strain induced martensitic transformation in the fracture structure of 316L and 316LN stainless steels was analyzed by X-ray diffraction analysis as shown in Fig. 10. There is some martensite transformation at the crack tip in both alloys, as shown in Fig. 10. The quantity of martensitic transformation is dependent on the temperature of the fatigue test. As the temperature increases, the quantity of phase transformation decreases. A larger amount of transformed martensite is formed at 25°C than at 600°C in both alloys.

Based on the consideration of the peaks of (211) plane in Fig. 10, a similar amount of martensitic transformation was induced during the fatigue test. In fact, it is a little difficult to quantify the amount of the

martensite phase transformation because the fracture surface areas on which the X-ray diffraction tests were carried out are not within the exact same stress intensity factor range in all tested alloys. So it is difficult to compare the amount of transformed martensite phase in the tested alloys directly from Fig. 10. But it can be considered that there is no significant difference in the amount of strain induced martensitic transformation in both 316L and 316LN stainless steels. Of course, there is some strengthening effect induced by martensite transformation. However, it seems that strain induced martensitic transformation is not the critical factor for the difference in the fatigue crack growth rate of 316L and 316LN stainless steels.

4.3. Effect of dislocation structure in the fatigue plastic zone

Fatigue crack growth is basically material degradation due to a slip in the cyclic plastic strain zone. So the deformation behavior in the cyclic plastic strain zone influences the fatigue crack growth resistance of materials. TEM observations were carried out to investigate the deformation behavior in the cyclic plastic strain zone. Dislocations in 316L stainless steel have a tangled cellular structure while dislocations in 316LN stainless steel have a planar structure, as shown in Fig. 11. The dislocation structure in austenite stainless steel depends on the ease of cross slip. The planar arrangement of dislocations in the slip plane occurs when (1) the stacking fault energy of materials is low [15,16] and (2) there is short range order phase [17] in the alloys.

The fact that nitrogen addition to austenite stainless steel induces the planar arrangement of dislocations was reported also in other studies [3,18]. Swann [18] reported that N induces the planar arrangement of dislocations, and C promotes the cellular arrangement of dislocations in N or C added austenite stainless steel. Vogt [3] observed that dislocation arrangement transforms to a planar structure, and fatigue crack growth rate decreases from 77 to 300 K when nitrogen was added to 0.2% N in stainless steel. The fact that N addition to stainless steel promotes the planar arrangement of dislocation in the fatigue plastic zone is a trend agreed upon by various investigators.

The significant difference between 316L and 316LN stainless steels during the fatigue crack growth test is the dislocation structure in the cyclic plastic strain zone. The planar arrangement of dislocation means that it is more difficult to cross slip in 316LN stainless steel than in 316L stainless steel. So it is considered that the difficulty to cross slip in 316LN stainless steel improves the resistance to fatigue crack growth of 316LN stainless steel more than of 316L stainless steel.

5. Conclusions

1. Nitrogen added 316LN stainless steel (0.14% N) has better resistance to fatigue crack growth than 316L stainless steel at room temperature and 600°C.
2. The better fatigue crack growth resistance of 316LN stainless steel is related to the planar slip characteristic in the fatigue plastic zone rather than the martensitic transformation at the crack tip or crack closure.

References

[1] K.J. Irvine, D.T. Llewellyn, F.B. Pickering, J. Iron Steel Inst. 199 (1961) 153.
[2] K.J. Irvine, T. Gladman, F.B. Pickering, J. Iron Steel Inst. 207 (1969) 1017.
[3] J.B. Vogt, J. Foct, C. Regnard, G. Robert, J. Dhers, Metall. Trans. A 22A (1991) 2385.
[4] R.E. Stoltz, J.B. Vander Sande, Metall. Trans. A 11A (1980) 1033.
[5] J.O. Nilsson, J.B. Vander Sande, Mater. Struct. 7 (1) (1984) 55.
[6] R. Sandstrom, H. Bergquist, Scand. J. Metall. 6 (1997) 156.
[7] G.T. Hahn, R.G. Hoagland, A.R. Rosenfield, Metall. Trans. 3 (1972) 1189.
[8] F.L. Liang, C. Laird, Mater. Sci. Eng. A 117 (1989) 95.
[9] G.R. Chanani, S.D. Antolovich, Metall. Trans. 5 (1974) 217.
[10] A. Pineau, L.F. van Swam, R.M. Pelloux, Scr. Metall. 7 (1973) 657.
[11] M. Bayerlein, H.J. Christ, H. Mughrabi, Mater. Sci. Eng. A 114 (1989) L11.
[12] A.K. Head, Philos. Mag. 44 (7) (1953) 925.
[13] W. Elber, ASTM STP 486, American Society for Testing and Materials, 1971, p. 230.
[14] S. Ganesh Sundara Raman, K.A. Padmanabhan, Mater. Sci. Technol. 10 (1994) 614.
[15] R.E. Schramm, R.P. Reed, Metall. Trans. A. 6A (1975) 1245.
[16] R.E. Stoltz, J.B. Vander Sande, Metall. Trans. A. 11A (1980) 1033.
[17] V. Gerold, H.P. Karnthaler, Acta Metall. 37 (1989) 2177.
[18] P.R. Swann, Corrosion 19 (1963) 102.